Revision_1

On the labyrinthine world of arsenites: A single-crystal neutron and X-ray diffraction study of cafarsite

G. Diego Gatta[1,2], Nicola Rotiroti[1], Fernando Cámara[1], Martin Meven[3]

[1] Dipartimento di Scienze della Terra, Università degli Studi di Milano, Via Botticelli 23, I-20133 Milano, Italy
[2]CNR - Istituto di Cristallografia, Via G. Amendola 122/o, Bari, Italy
[3]Institute of Crystallography, RWTH Aachen University, and Jülich Centre for Neutron Science (JCNS) at Heinz Maier-Leibnitz Zentrum (MLZ), Lichtenbergstraße 1, D-85747 Garching, Germany

Running title: Crystal chemistry of cafarsite

Corresponding author: G. Diego GATTA

Dip. Scienze della Terra
Universita' degli Studi di Milano
Via Botticelli, 23
I-20133 Milano, Italy
Tel. +39 02 503 15607
Fax +39 02 503 15597
E-Mail: diego.gatta@unimi.it

(To be submitted to *Physics and Chemistry of Minerals*)

On the labyrinthine world of arsenites: A single-crystal neutron and X-ray diffraction study of cafarsite

G. Diego Gatta[1,2], Nicola Rotiroti[1], Fernando Cámara[1], Martin Meven[3]

[1] Dipartimento di Scienze della Terra, Università degli Studi di Milano,
Via Botticelli 23, I-20133 Milano, Italy
[2]CNR - Istituto di Cristallografia, Via G. Amendola 122/o, Bari, Italy
[3]Institut für Kristallographie, RWTH Aachen, and Jülich Centre for Neutron Science (JCNS) at Heinz Maier-Leibnitz Zentrum (MLZ), Lichtenbergstraße 1, D-85748 Garching, Germany

Abstract

The crystal chemistry of a cafarsite sample from the fengitic orthogneisses of the Mt. Leone-Arbola nappe (Lower Penninic), forming the central body of Mount Cervandone and cropping out both in Switzerland and Italy (Alpe Devero area, Verbano-Cusio-Ossola province), was investigated by electron microprobe analysis in wavelength-dispersive mode (EPMA-WDS), single-crystal Raman spectroscopy, and single-crystal X-ray and neutron diffraction at 293 K. The sample of cafarsite of this study was found experimentally to be anhydrous and the chemical formula obtained on the basis of the EPMA-WDS data and structural refinements is the following: $^{Ca1,Ca2}(Ca_{15.56},Na_{0.44})_{\Sigma 16}{}^{Fe1}(Na_{0.53},Fe^{2+}_{0.17}REE_{0.30})_{\Sigma 1.00}{}^{Mn1,Ti,Fe2}(Mn_{0.85},Fe^{2+}_{3.20},Fe^{3+}_{4.47},Al_{0.11},Ti_{7.46})_{\Sigma 16.11}{}^{As1,As2,As3}(AsO_3)_{28}{}^{F}F$, with the general chemical formula $Ca_{16}(Na,Fe^{2+},REE)(Mn,Fe^{2+},Fe^{3+},Al,Ti)_{16}(AsO_3)_{28}F$ [or $Ca_{16}(Na,Fe^{2+},REE)(Ti,Fe^{3+},Al)_{12}(Fe^{2+},Mn)_4(AsO_3)_{28}F$]. Our experimental findings show that fluorine, which was unconsidered in the previous studies, is a key element. The anhydrous nature of this sample is also confirmed by its Raman spectrum, which does not show any evidence of active bands ascribable to the O-H stretching region. The X-ray and neutron structure refinements provide a structure model that is partially in agreement with the previous experimental findings. The space group (*i.e.*, *Pn*3) and the unit-cell constant (*i.e.*, 15.9507(4) Å) are conform to the literature data, but the structure of cafarsite, here refined, contains the following building units: 3 independent AsO_3-groups (trigonal pyramids), 1 CaO_6F polyhedron, 1 CaO_8 polyhedron, 2 independent $(Ti,Fe)O_6$ octahedra, 1 $(Na,Fe,REE)O_8$ polyhedron, and 1 $(Mn,Fe)O_6$ octahedron. Connections among polyhedra are mainly due to edge- or vertex-sharing; the AsO_3-groups are not connected to each other.

Keywords: cafarsite; arsenites; single-crystal X-ray and neutron diffraction; Raman spectroscopy; cation partitioning.

Introduction

Cafarsite is a rare mineral. It was discovered on the North-West side of Mount Cervandone (Binntal, Wallis, Switzerland). The species was first described by Graeser (1966) and ascribed to the arsenate class of minerals with the following chemical formula: $Ca_{5.5}Fe_{3.3}Mn_{1.7}Ti_{2.5}(AsO_4)_{12}\cdot 4H_2O$. Cafarsite forms mainly octahedral crystals, showing faces of cube and dodecahedron up to 3 cm in length. If not altered, cafarsite is dark brown in color with a strong vitreous luster, and is translucent red in thin grains (Graeser 1966). When altered, crystals usually show an external crust of pale brown color and earthy look. Frequently, altered cafarsite crystals are overgrown by agardite-(Y). On the basis of Weissenberg X-ray single-crystal data, Graeser (1966) described cafarsite as a cubic mineral, with a unit-cell length of approximately 16.0 Å and the potential space group *Pn*3.

The crystal structure of a cafarsite, with chemical formula $(Ca_{6.35}Mn_{0.79}Na_{0.77})(Ti_{3.81}Sn_{0.02}Al_{0.30}Fe_{2.34})As_{12.01}O_{36}\cdot 1.92H_2O$, was later solved and refined by Edenharter et al. (1977) on the basis of Weissenberg X-ray intensity data, in the space group *Pn*3 (with $a \approx 15.98$ Å). Based on their experimental findings, Edenharter et al. (1977) reclassified the mineral cafarsite as an oxide belonging to the hydroxide subclass, 4.JC.05 arsenites (Strunz and Nickel 2001). The structure of cafarsite was refined with two independent Ca sites (one with coordination number CN=6, the second with CN=8), one Ti site (with CN=6), one Mn site (CN=6), one Mn/Fe site (CN=6), one site occupied by Fe with an unusual 4-fold planar coordination environment (CN=4, square), and three independent As sites, each one connected to three oxygen atoms (with a trigonal pyramid coordination environment). The inter-polyhedral connection is based mainly on corner- or edge-sharing. However, the study of Edenharter et al. (1977) contains some weak points: the final agreement indexes of the structure refinement were significantly high (*i.e.*, R_1 = 8%, R_{all} = 12%) and the H_2O sites were not unambiguously located in the structure refinement. This led to an ambiguous knowledge of the crystal chemical formula of this mineral and to a completely unknown role played by the protons, and by their H-bonds, into the structure.

A more recent study on cafarsite from Binntal (Switzerland) was performed by Kloprogge and Frost (1999) by single-crystal Raman spectroscopy. However, the spectra were collected in the region between 150 and 1050 cm^{-1} and the active Raman bands pertaining to the O-H stretching region were not reported, leaving open questions about the hydrous nature of the cafarsite sample investigated. In addition, no chemical or crystallographic characterization was performed on the sample used in their study (Kloprogge and Frost 1999).

Inexplicably, the ideal chemical formula of cafarsite is reported in several databases as: $Ca_8(Ti,Fe^{2+},Fe^{3+},Mn)_{6\text{-}7}(AsO_3)_{12}\cdot 4\text{-}5H_2O$ (*e.g.*, *American Mineralogist Crystal Structure Database Record*, http://rruff.info/doclib/hom/cafarsite.pdf; Fleischer et al. 1978).

Based on the several open questions left by the previous studies of Graeser (1966), Edenharter et al. (1977) and Kloprogge and Frost (1999), the aim of this study was a reinvestigation of the crystal chemistry of cafarsite in order to provide: *i)* a reliable structure model with a full description of the cation partitioning and *ii)* an unambiguous location of the proton sites, for a full description of the atomic relationship via the H bond. To achieve this goal, we used electron microprobe analysis in wavelength-dispersive mode (EPMA-WDS), single-crystal Raman spectroscopy, and single-crystal X-ray (SCXRD) and neutron diffraction (SCND). This study was performed in the framework of a series of studies devoted to understand the labyrinthine world of hydrous minerals, mainly based on single-crystal neutron diffraction (*e.g.*, Gatta et al. 2015, 2016a,b, 2017).

Experimental methods

For this multi-methodological study, we selected a non-altered dark brown octahedron of cafarsite (9 mm), semitransparent and with strong vitreous luster coming from the Wannigletscher (North-West side of Monte Cervandone, Binntal, Switzerland, and type locality for the mineral). The mineral was found in the fengitic orthogneisses belonging to the Mount Leone-Arbola nappe (Lower Penninic), forming the central body of Mount Cervandone and cropping out both in Switzerland and Italy (Alpe Devero area, Verbano-Cusio-Ossola province).

1)_Chemical analysis

The chemical composition of cafarsite by EPMA-WDS was obtained using a Jeol JXA-8200 electron microprobe at the Earth Science Department of the University of Milano (ESD-UMI). The crystal fragment (approximately 2 mm^3) was mounted in epoxy resin, polished and carbon coated. Major and minor elements were determined at 15 kV accelerating voltage, 5 nA beam current, and 5 μm beam diameter with a counting time of 30 sec on the peaks and 10 sec on the backgrounds. The following elements were analysed: As, Ti, Al, Ce, La, Fe, Mn, Ca, Na, and F using a series of well characterized minerals and glasses as standards (ilmenite for Ti, realgar for As, grossular for Al, Ce-phosphate glass for Ce, La-phosphate glass for La, fayalite for Fe, rhodonite for Mn, gossular for Ca, omphacite for Na, fluor-hornblende for F). P, Si, Mg, Ba, Sr, and K were sought for but not detected. Arsenic is one of the dominant elements in cafarsite (~ 55 wt% As_2O_3). Two different minerals were actually tried as standards for As: nickeline and realgar. Using nickeline, the fraction

of As was significantly lower than the expected one; using realgar, the fraction was closer to the ideal one but still slightly lower than that expected one (*i.e.*, ~ 52.5 wt% As_2O_3, Table 1). Even an uncertainty of 5-10% on the measured weight fraction of As_2O_3 can have a drastic effect on the final chemical formula. The raw data were corrected for matrix effects using a *CITZAF* routine available in the Jeol suite of programs. A total number of 10 point analyses were performed. The crystal was found to be homogeneous within the analytical error. The average chemical composition and the proportional formula are given in Table 1.

2)_Single-crystal X-ray and neutron diffraction experiments

A single crystal of cafarsite (0.29 x 0.21 x 0.18 mm^3), optically homogeneous and free of inclusions under a transmitted-light polarizing microscope, was selected for the X-ray diffraction experiment. X-ray intensity data were collected at room temperature and up to $2\theta_{max} = 72.4°$ (d_{min} ~ 0.6 Å, with $-24 \leq h \leq +25$, $-24 \leq k \leq +24$ and $-25 \leq l \leq +25$, Table 2) with an Xcalibur - Oxford Diffraction diffractometer at the ESD-UMI, equipped with a CCD, monochromatized Mo-$K\alpha$ radiation and operated at 50 kV and 30 mA. The X-ray data collection was performed with a combination of φ/ω scans, step size of 1° and an exposure time of 5 s/frame. A total number of 108,931 Bragg reflections (with a high degree of redundancy) were collected, out of which 2612 were unique and 1958 with $I_o > 3\sigma(I_o)$ (Table 2), giving a metrically cubic unit-cell with: a = 15.9507(4) Å. The reflection conditions suggested the space group *Pn*3, as previously reported by Graeser (1966) and Edenharter et al. (1977). The intensity data were then integrated and corrected for Lorentz-polarization effects, using the computer program CrysAlis (Agilent Technologies 2012). An analytical absorption correction was applied by Gaussian integration based upon the physical description of the crystal (using CrysAlis, Agilent Technologies 2012). After the corrections, the discrepancy factor among symmetry-related reflections (Laue class: *m*-3) was R_{eq} = 0.0408 (Table 2).

A suite of crystals was sorted out for the neutron diffraction experiment. After a preliminary check, a monochromatic single-crystal neutron diffraction experiment was performed on a crystal of cafarsite (3.1 x 3.0 x 2.7 mm^3) using the diffractometer HEiDi at the hot source (fast neutrons) of the neutron source FRM II of the Heinz Maier-Leibnitz-Zentrum (MLZ), Germany. A first set of diffraction data was collected at room temperature with a wavelength of the incident beam of 1.170(1) Å (Ge-311 monochromator, Er foil to suppress λ/3 contamination) up to $2\theta_{max} = 122°$ ($\sin(\theta)/\lambda = 0.75$ $Å^{-1}$). A second set of intensity data was collected at higher $\sin(\theta)/\lambda$ up to 0.89 $Å^{-1}$ with a wavelength of the incident beam of 0.7925(5) Å (Ge-422 monochromator, Er foil to suppress

λ/2 contamination). The diffractometer is equipped with a ^{3}He single counter detector for high sensitivity down to short wavelengths. In total 8306 reflections were collected up to $d_{min} \sim 0.7$ Å (with $-23 \leq h \leq +25$, $-23 \leq k \leq +25$ and $-25 \leq l \leq +25$, Table 2), using pure ω-scan, ω-θ scan and ω-2θ scan strategy as reported in Table 2, out of which 2955 were unique and 1521 with $I_o > 3\sigma(I_o)$. Integrated intensities were then corrected for the Lorentz effect; absorption correction was found to be negligible. After the corrections, the discrepancy factor among symmetry-related reflections (Laue class: *m*-3) was $R_{eq} = 0.0511$ (Table 2).

Further details pertaining to the X-ray and neutron data collections are given in Table 2.

3)_Raman spectroscopy

A crystal of cafarsite was used for the Raman investigation at the Laboratory for Provenance Studies of the University of Milano-Bicocca, Department of Earth and Environmental Sciences. Single-crystal Raman spectra were collected using a Reinshaw QONTOR confocal micro-Raman spectrometer, equipped with a charge-coupled detector. Spectra were collected by exciting the sample with a 532 nm laser. The laser beam was focused on the sample on a spot with nearly 2 μm diameter (objective 50×). Spectra were collected in backscattering geometry in the range 150–4000 cm^{-1}, with 0.4 s counting time and 200 accumulations. Positions of the Raman bands were measured using a Gauss-Lorentzian deconvolution procedure, with an accuracy of 0.5 cm^{-1}. The representative Raman spectrum is shown in Fig. 1.

Results: X-ray and neutron structure refinement

The X-ray and neutron intensity data collected at 293 K were first processed in order to calculate the normalized structure factors (*E*'s) and their statistical distributions, using the program E-STATISTICS, implemented in the WinGX package (Farrugia 1999). The structure was found to be centrosymmetric (with >90% likelihood), processing both the datasets.

X-ray and neutron anisotropic structure refinements were then performed in the space group *Pn*3 using the JANA2006 software (Petříček et al. 2014), starting from the (H-free) structure model of Edenharter et al. (1977). The X-ray scattering factors and the neutron scattering lengths of Ca, Mn, Fe, Ti, As, O and F were used according to the *International Tables for Crystallography Vol. C*, as implemented in JANA2006. The effects of secondary isotropic extinction (B-C type 1 Gaussian isotropic) were corrected following the formalism of Becker and Coppens (1974), as implemented in JANA2006. The structure model of Edenharter et al. (1977) was found to be only

partially consistent with the data of this study. After a series of structure refinement cycles and inspection of the difference-Fourier maps of the electron (for X-ray structure refinement) and nuclear (for neutron refinement) density functions, the structure model with the highest figure of merit was obtained with:

1) Three independent As sites with full site occupancies, here labelled as *As1*, *As2* and *As3* (Table 3);
2) Two independent Ca sites, here labelled as *Ca1* and *Ca2* (Table 3). However, the X-ray structure refinement shows that the *Ca1* site can be potentially split in two mutually exclusive sub-sites (*Ca1a* and *Ca1b*, Table 3);
3) One independent site at *x*, 3/4, 1/4, here labelled as *Ti*, which is populated by Ti (dominant) and Fe (subordinate) (Table 3);
4) One site at 1/4, 3/4, 3/4, here labelled as *Fe1*, which is partially populated by Fe (Table 3) and likely also by Na and REE, as suggested by the EPMA-WDS data (Table 1);
5) One site at *x*, 1/4, 1/4, here labelled as *Fe2* site, which is populated by Fe and Ti (Table 3) and likely also by Al, as suggested by the EPMA-WDS data (Table 1);
6) One site at 0, 0, 0, here labelled as *Mn1*, which is populated by Fe (dominant) and Mn (subordinate) (Table 3);
7) Seven independent oxygen sites, here labelled as *O1*-*O7* (Table 3);
8) One independent fluorine site, here labelled as *F* at 3/4, 3/4, 3/4 with full site occupancy (Table 3).

Modelling the site populations at the *Fe1*, *Fe2*, *Mn1* and *Ti* site was not trivial, especially because Mn (-3.73 fm) and Ti (-3.438 fm) have negative neutron scattering lengths whereas Fe (9.45 fm) has a positive one (potentially generating weak effective scattering lengths on the corresponding mixed sites). This, on the other hand, provided a complementary picture to that obtained by the X-ray refinement, leading to the aforementioned structure model which is consistent for both (*i.e.*, neutron *and* X-ray) refinements. The site-labelling scheme was kept as similar as possible to that previously used by Edenharter et al. (1977). When convergence was achieved, no residual peaks were found in the difference-Fourier maps of the electron or nuclear density potentially ascribable to H sites. As fluorine and oxygen have similar X-ray scattering factors and neutron scattering lengths, the *F* site was unambiguously located on the basis of its bond valence value, which was approximately 1 *v.u.*. All the other O sites showed valence units values close to 2 (Table 3).

When the final cycles of anisotropic refinements were conducted, convergence was achieved with no significant correlation among the refined parameters in the variance-covariance matrix. No peaks larger than -1.0/+1.7 *e*-/Å^3 and -3.4/+2.4 fm/Å^3 were found in the final difference-Fourier

maps of the electron and nuclear density functions, respectively (Table 2). The final agreement index of the X-ray structure refinement $R(F)$ was 0.0208 for 123 refined parameters and 1958 unique reflections with $Io>3\sigma(Io)$ (XRDSC-1, Table 2), whereas for the neutron structure refinement $R(F)$ = 0.0531 for 113 refined parameters and 1521 unique reflections with $Io>3\sigma(Io)$ (NDSC, Table 2). Atomic coordinates and displacement parameters are listed in Tables 3 and 4; relevant bond lengths and angles are listed in Table 5.

As the structure of cafarsite showed evidence of site positional disorder, which will be later discussed, a further structure refinement was conducted on the basis of the X-ray data with the *Fe1* site at *x*, 3/4, 3/4 (rather that at 1/4, 3/4, 3/4) and the following couples of mutually exclusive sub-sites: *Ca1a* and *Ca1b*, *O5* and *O5'*, *O7* and *O7'* (XRDSC-2, Tables 2-5). However, the quality of the refinement was not significantly higher if compared to the previous one (*i.e.*, XRDSC-1, Tables 2-5).

Discussion

The chemical composition of the cafarsite sample of this study from Mt. Leone-Arbola nappe – Mt. Cervandone, Italy, based on EPMA-WDS analysis, shows a significant difference if compared to that reported by Graeser (1966) (*i.e.*, $Ca_{5.5}Fe_{3.3}Mn_{1.7}Ti_{2.5}(AsO_4)_{12}\cdot 4H_2O$, in orthogneisses of the Mt. Leone nappe, southern Binnatal, Switzerland) and by Edenharter et al. (1977) (*i.e.*, $(Ca_{6.35}Mn_{0.79}Na_{0.77})(Ti_{3.81}Sn_{0.02}Al_{0.30}Fe_{2.34})As_{12.01}O_{36}\cdot 1.92H_2O$, from the same rock sample of Graeser 1966): the sample of this study is nominally anhydrous, with the following chemical formula: $Ca_{15.56},Na_{0.97},REE_{0.30},Mn_{0.85},Fe^{2+}_{3.37},Fe^{3+}_{4.47},Al_{0.11},Ti_{7.46}(AsO_3)_{28}$ F (Table 1), and ideal chemical formula: $Ca_{16}(Na,Fe^{2+},REE)(Mn,Fe^{2+},Fe^{3+},Al,Ti)_{16}(AsO_3)_{28}F$ [or $Ca_{16}(Na,Fe^{2+},REE)(Ti,Fe^{3+},Al)_{12}(Fe^{2+},Mn)_4(AsO_3)_{28}F$]. On the basis of the EPMA-WDS data and of the experimental findings of the X-ray and neutron structure refinements, the crystal chemical formula of the cafarsite sample of this study is:

$^{Ca1,Ca2}Ca_{16}\,^{Fe1}(Na,Fe^{2+},REE)\,^{Mn1,Fe2,Ti}(Ti^{4+},Fe^{3+},Mn^{2+},Fe^{2+},Al)_{16}\,^{As1,As2,As3}(As^{3+}O_3)_{28}\,^{F}F$.

The nominally anhydrous nature of this sample is also confirmed by its Raman spectrum (Fig. 1), which does not show any evidence of active bands ascribable to the O-H stretching region. The presence of arsenite groups in the cafarsite structure, reported by Edenharter et al. (1977), is here confirmed, as well as the presence of Ca, Na, Fe, Mn, Ti, and REE as principal elements along with F.

The (un-oriented) Raman spectrum collected in this study (150–4000 cm^{-1}, Fig. 1) is in general agreement with that reported by Kloprogge and Frost (1999), though the previous one was restricted to the range between 150 and 1050 cm^{-1}, and it is virtually identical to that reported in the

RRUFF database (200 – 6000 cm^{-1}, un-oriented sample #R080118, http://rruff.info/Cafarsite; Lafuente et al. 2015). Even the spectrum of the cafarsite sample #R080118 reported in the RRUFF database does not show evidence of active bands ascribable to the O-H stretching region. As shown by Kloprogge and Frost (1999), a strong effect of the crystal orientation on the intensity of the Raman bands occurs, which affect mainly the bands with wavenumber between 150 and 400 cm^{-1}. A careful analysis of the Raman active bands ascribable to Ca-O, Fe-O, Ti-O, Mn-O and As-O modes is provided in Kloprogge and Frost (1999).

The X-ray and neutron structure refinements of the cafarsite sample of this study are mutually consistent and provide a structure model that is only partially consistent with that of Edenharter et al. (1977). In particular, the structure of cafarsite, here refined, contains the following building units: 3 independent AsO_3-groups (trigonal pyramids), 1 CaO_6F polyhedron, 1 CaO_8 polyehdron, 2 independent $(Ti,Fe)O_6$ octahedra, 1 $(Na,Fe,REE)O_4O_4$ polyhedron, and 1 $(Mn,Fe)O_6$ octahedron. The bonding scheme among the polyhedra can be deduced in Fig. 2, in which it is shown that connections are mainly due to edge- or vertex-sharing. The AsO_3-groups are not connected to each other. The *Fe*1 site, reported by Edenharter et al. (1977) to have an unusual 4-fold planar coordination environment (CN = 4, square), actually has a 4+4 coordination (*i.e.*, $^{Fe1}(Na,Fe,REE)O_4O_4$ polyhedron), with 4 shorter (~2.2 Å) and 4 longer (~2.8 Å) *M*-O bond lengths (Table 5).

The pronounced anisotropic displacement parameters of some atomic sites, here also modelled with *Ca1a*-*Ca1b*, *O5*-*O5'* and *O7*-*O7'* subsites only 0.2-0.3 Å apart (Tables 3, 4 and 5), are indicative of a severe (static) positional disorder of the atomic sites in the structure of cafarsite. Any attempt to reduce the disorder by lowering the symmetry was unsuccessful, consistently with the fact that the isometric nature of the unit-cell, reflection conditions and statistical distributions of the normalized structure factors converge to the space group *Pn*3; in other words, the disorder is "real". The multi-element population at the principal cationic sites somehow promote the disordering, which is less pronounced in sites in which the substituents have similar *M*-O bond distances, but can be severe when the substituents promote a different bonding scheme (*e.g.*, Na, Fe^{2+} and REE at the *Fe1* site, Tables 1, 3, 4 and 5), leading to a local displacement of the coordinated oxygen atoms.

A question is still open: can cafarsite be a hydrous mineral, as previously reported, or not? Our experimental findings show, unambiguously, that the sample used in this study is actually anhydrous and that fluorine, which was overlooked in the previous studies, is a key element. The previous experimental findings of Graeser (1966), Edenharter et al. (1977) and Kloprogge and Frost (1999) did not provide an unambiguous evidence of the presence of H_2O (in its molecular form or

as hydroxyl group) in the structure of cafarsite. The only chemical analysis was reported by Graeser (1966), with a H_2O fraction of 2.4 wt%; Edenharter et al. (1977) worked on material provided by Graeser (likely from the same rock sample previously used, which overall contained only 1.6 wt% of H_2O) and Kloprogge and Frost (1999) did not perform any chemical characterization of their natural sample. In addition, as reported above, even the Raman spectrum of the cafarsite sample #R080118 in the RRUFF database does not show evidence of active bands ascribable to the O-H stretching modes. However, a further study on a natural sample was performed by Boscardin and Mattioli (1981) by means of infrared spectroscopy, reporting that eroded crystals of cafarsite show strong hydration phenomena, as reflected by new IR-active bands at 3410 and 1635 cm^{-1} not observed in well preserved crystals.

Overall, we are inclined to believe that cafarsite grows as an anhydrous mineral but it could be easily altered, likely to a hydrous form. In fact, there is a severe change in color and opacity among crystals available in private or public collections, indicative of a different alteration state. This would explain why, in the open literature, cafarsite was assumed to be a hydrous species after Graeser (1966). The inexplicable chemical formula of cafarsite reported in several databases as $Ca_8(Ti,Fe^{2+},Fe^{3+},Mn)_{6\text{-}7}(AsO_3)_{12}\cdot 4\text{-}5H_2O$, which does not derive from the previous results of Graeser (1966) and Edenharter et al. (1977), should be reconsidered, especially due to the experimental findings of this multi-methodological study. An additional source of confusion is that, in several databases (among those even RRUFF: http://rruff.info/Cafarsite), the sample of cafarsite used by Edenharter et al. (1977) for the structure solution is erroneously described as "synthetic"; the sample used by Edenharter et al. (1977) is natural and was kindly provided by Graeser (1966), as clearly stated in their manuscript (*"Aus mehreren kleinen Kristallen und Bruchstücken von Cafarsit, die uns St. Graeser freundlicherweise zur Varfügug stellte..."*).

Acknowledgements

The authors acknowledge the Heinz Maier-Leibnitz Zentrum (MLZ) in Garching, Germany, for the allocation of neutron beam time at the single crystal diffractometer HEIDI operated by RWTH Aachen University and Jülich Centre for Neutron Science, Forschungszentrum Jülich (JARA cooperation). The authors thank P. Vignola, who kindly provided the sample of cafarsite used in this study, and the staff of the Laboratory for Provenance Studies of the University of Milano-Bicocca, Department of Earth and Environmental Sciences, for the Raman experiments. Two anonymous reviewers are thanked.

References

Agilent (2012) CrysAlis computer program, Agilent Technologies, XRD Products.

Becker PJ, Coppens P (1974) Extinction within the limit of validity of the Darwin transfer equations. I. general formalisms for primary and secondary extinction and their application to spherical crystal. *Acta Crystallogr* A30:129–147.

Boscardin M, Mattioli V (1981) Mte. Cervandone: Die seltenen Arsenmineralien aus den alpinen Klüften des Mte. Cervandone. *Lapis* 6:30-32.

Edenharter A, Nowacki W, Weibel M (1977) Zur struktur und zusammensetzung von cafarsit, cafarsit ein As(III)-oxid, kein arsenat. *Schweiz Mineral Petrogr Mitt* 57:1-16

Farrugia LJ (1999) WinGX suite for small-molecule single-crystal crystallography. *J Appl Crystallogr* 32:837-838.

Fleischer M, Pabst A, White J S (1978) New mineral names. *Am Mineral* 63:793-796.

Gatta GD, Redhammer GJ, Vignola P, Meven M, McIntyre GJ (2015) Single-crystal neutron diffraction and Mössbauer spectroscopic study of hureaulite, $(Mn,Fe)_5(PO_4)_2(HPO_4)_2(H_2O)_4$. *Eur J Mineral* 28:93-103.

Gatta GD, Redhammer GJ, Guastoni A, Guastella G, Meven M, Pavese A (2016a) H-bonding scheme and cation partitioning in axinite: a single-crystal neutron diffraction and Mössbauer spectroscopic study. *Phys Chem Minerals* 43:341–352.

Gatta GD, Bosi F, Fernandez-Diaz MT, Hålenius U (2016b) H-bonding scheme in allactite: a combined single-crystal X-ray and neutron diffraction, optical absorption spectroscopy, FTIR and EPMA-WDS study. *Mineral Mag* 80:719-732.

Gatta GD, McIntyre GJ, Oberti R, Hawthorne FC (2017) Order of $^{[6]}Ti^{4+}$ in a Ti-rich calcium amphibole from Kaersut, Greenland: a combined X-ray and neutron diffraction study. *Phys. Chem. Minerals* 44:83-94.

Graeser S (1966) Asbecasit und Cafarsit, zwei neue Mineralien aus dem Binnatal (Kt. Wallis). *Schweiz Mineral Petrogr Mitt* 46:367-375.

Kloprogge JT, Frost RL (1999) Raman Microscopy Study of Cafarsite. *Appl Spectrosc* 53:874-880.

Lafuente B, Downs RT, Yang H, Stone N (2015) The power of databases: the RRUFF project. In: Highlights in Mineralogical Crystallography, T Armbruster and RM Danisi, eds., Berlin, Germany, De Gruyter, pp. 1-30.

Petříček V, Dušek M, Palatinus L (2014) Crystallographic Computing System JANA2006: General features. *Z Kristallogr* 229:345–352.

Strunz H, Nickel EH (2001) Strunz mineralogical tables. Schweizerbart, Stuttgart, 869 p.

Table 1. Representative composition of the cafarsite from Mt. Leone-Arbola nappe – Mt. Cervandone, Italy, based on EPMA-WDS analysis (average of 10 data points). *A-1*: chemical analysis with the measured As_2O_3 fraction; *A-2*: chemical analysis with the calculated As_2O_3 fraction assuming 28 As *a.p.f.u.*. FeO and Fe_2O_3 recalculated on the basis of crystal chemical constraints. The chemical formulae are calculated on the basis of 85 (equivalent) oxygen atoms and the structure model reported in Table 3.

	A-1 Wt%	*A-2 Wt%*		*A-1 a.p.f.u.*	*A-2 a.p.f.u.*
Al_2O_3	0.11	0.11	As^{3+}	27.24	28.00
TiO_2	11.94	11.94			
FeO_{TOT}	11.29	11.29	Ti^{4+}	7.69	7.46
FeO	5.42	4.85	Al	0.11	0.11
Fe_2O_3	6.52	7.15	Fe^{3+}	4.20	4.47
MnO	1.21	1.21	Fe^{2+}	3.88	3.37
As_2O_3	52.37	55.50	Mn^{2+}	0.88	0.85
CaO	17.48	17.48	Σ	16.76	16.25
Na_2O	0.60	0.60			
La_2O_3	0.29	0.29	Na	1.00	0.97
Ce_2O_3	0.69	0.69	Ca	16.04	15.56
F	0.38	0.38	La	0.09	0.09
TOTAL	97.01	100.21	Ce^{3+}	0.22	0.21
O=F	0.16	0.16	Σ	17.35	16.83
TOTAL	96.85	100.05			
			Σ TOTcat.	34.11	33.08
			F	1.03	1.00

A-1:

$^{Ca1,Ca2}Ca_{16.04}{}^{Fe1}(Na_{1.00},REE_{0.31})_{\Sigma 1.31}{}^{Mn1,Fe2,Ti}(Mn_{0.88},Fe^{2+}{}_{2.88},Fe^{3+}{}_{4.20},Al_{0.11},Ti_{7.69})_{\Sigma 16.76}{}^{As1,As2,As3}(AsO_3)_{27.24}{}^{F}F_{1.03}$

A-2:

$^{Ca1,Ca2}(Ca_{15.56},Na_{0.44})_{\Sigma 16}{}^{Fe1}(Na_{0.53},Fe^{2+}{}_{0.17}REE_{0.30})_{\Sigma 1.00}{}^{Mn1,Ti,Fe2}(Mn_{0.85},Fe^{2+}{}_{3.20},Fe^{3+}{}_{4.47},Al_{0.11},Ti_{7.46})_{\Sigma 16.11}{}^{As1,As2,As3}(AsO_3)_{28}{}^{F}F$

Table 2. Data pertaining to the single-crystal X-ray (XRDSC-1 and XRDSC-2, see also Table 3) and neutron (NDSC) data collection and structure refinements of cafarsite.

	XRDSC-1	XRDSC-2	NDSC
T (K)	293	293	293
Crystal size (mm)	0.29 x 0.21 x 0.18	0.29 x 0.21 x 0.18	3.1 x 3.0 x 2.7
Radiation	Mo-$K\alpha$	Mo-$K\alpha$	Neutron constant wavelengths: *A*: λ=1.170(2) Å, *B*: λ=0.7925(5) Å
Reference formula	$Ca_{16}Fe(Ti,Fe,Mn)_{16}As_{28}O_{84}F$	$Ca_{16}Fe(Ti,Fe,Mn)_{16}As_{28}O_{84}F$	$Ca_{16}Fe(Ti,Fe,Mn)_{16}As_{28}O_{84}F$
Z	1	1	1
Scan details:			
λ, time/step, collimation,	5 s	5 s	*A*: 1 – 6 s, 60',
range, type, steps (u, v, q)	ω/φ-scan, 1°	ω/φ-scan, 1°	2θ<80°, ω-scan, 41 steps (17.4, -66, 79) 80°< 2θ<100°, ω-θ-scan, 31 steps (18, -65, 85) 100°<2θ<122°, ω-2θ scan, 25 steps (15, 0, 0) *B*: 2 – 8 s, 60', 2θ<76°, ω-θ scan, 35 steps (12.25, 0, 0)
Space Group	*Pn*3	*Pn*3	*Pn*3
a (Å)	15.9507(4)	15.9507(4)	15.9507(4)
d_{min} (Å)	0.6	0.6	0.7
h_{min}/h_{max}, k_{min}/k_{max}, l_{min}/l_{max}	-24/+25, -24/+24, -25/+25	-24/+25, -24/+24, -25/+25	-23/+25, -23/+25, -25/+25
Measured reflections	108,931	108,931	8306
Unique reflections	2612	2612	2955
Reflections with $I_O > 3\sigma(I_O)$	1958	1958	1521
R_{eq}	0.0410	0.0410	0.0511
N. of refined parameters	123	121	113
R(F), observed reflections	0.0208	0.0215	0.0531
wR(F), observed reflections	0.0241	0.0249	0.0388
R(F), all reflections	0.0358	0.0368	0.1662
GoF	1.43	1.48	1.62
Residuals (e-/Å^3, fm/Å^3)	-1.0/ +1.7	-0.9/ +1.7	-3.4/ +2.4

Notes: Structure refinements on *F*. $R_{eq}=\Sigma|F_o^2-F_o^2{}_{(mean)}|/\Sigma F_o^2$; $R=\Sigma||F_o|-|F_c||/\Sigma|F_o|$; $w=1/[\sigma^2(F_o)+(0.0001*F_o)^2]$. Unit-cell parameters based on single-crystal X-ray data. Isotropic extinction coefficient based on the formalism of Becker and Coppens (1974), as implemented in JANA2006. XRDSC-1 and XRDSC-2 represent two different X-ray refinements based on different protocols; details are given in the section *"Results: X-ray and neutron structure refinement"* and in Table 3. Some of the refined parameters were fixed in the last cycles of the XRDSC-2 refinement. Neutron diffraction scan width = $(u + v*\tan\theta + q*\tan^2\theta)^{0.5}$.

Table 3. Fractional atomic coordinates, site occupancy factors (*s.o.f.*, all expressed in *e*-, for comparison), bond valences of the anionic sites (*v.u.*, in Italics) and displacement parameters (Å^2) based on the X-ray (XRDSC) and neutron (NDSC) structure refinements. U_{eq} is defined as one third of the trace of the orthogonalized U_{ij} tensor (in Table 4); U_{iso} is the isotropic displacement parameter.

Site	*s.o.f. in e⁻, v.u.*	*x/a*	*y/b*	*z/c*	U_{eq}/U_{iso}
XRDSC-1					
As1	As, 33	0.37638(2)	0.37638(2)	0.37638(2)	0.00541(5)
As2	As, 33	0.22921(2)	0.97783(2)	0.03845(2)	0.00445(7)
As3	As, 33	0.39276(2)	0.64083(2)	0.35164(2)	0.00808(8)
Ca1a	Ca, 2.9(4)	0.1527(8)	0.1527(8)	0.1527(8)	0.0020(2)
Ca1b	Ca, 17.2(4)	0.1634(1)	0.1634(1)	0.1634(1)	0.0020(2)
Ca2	Ca, 20.2(4)	0.09341(3)	0.62515(3)	0.35629(3)	0.0064(1)
Ti	(Ti,Fe), 24.6(1)	0.95176(3)	0.75	0.25	0.0037(1)
Fe1	Fe, 22.6(1)	0.25	0.75	0.75	0.0330(5)
Fe2	Fe, 21.37(5)	-0.00609(4)	0.25	0.25	0.0023(2)
Mn1	(Mn,Fe), 25.5(1)	0	0	0	0.0052(2)
O1	O, 8, *1.937(6)*	-0.0055(1)	0.9813(1)	0.1370(1)	0.0075(5)
O2	O, 8, *1.738(5)*	0.3098(1)	0.0036(1)	0.3598(1)	0.0080(5)
O3	O, 8, *2.131(6)*	0.2878(1)	0.6330(1)	0.0476(1)	0.0082(5)
O4	O, 8, *2.021(6)*	0.1638(1)	0.7378(1)	0.1456(1)	0.0094(5)
O5	O, 8, *1.811(8)*	0.1740(1)	0.5948(2)	0.2225(2)	0.043(1)
O6	O, 8, *2.211(7)*	0.0324(1)	0.6639(1)	0.2256(1)	0.0084(5)
O7	O, 8, *1.796(7)*	0.1733(1)	0.4177(1)	0.2134(1)	0.0208(7)
F	F, 8.5(2), *0.831(3)*	0.75	0.75	0.75	0.0096(10)
XRDSC-2					
As1	As, 33	0.37639(2)	0.37639(2)	0.37639(2)	0.00540(5)
As2	As, 33	0.22920(2)	0.97784(2)	0.03845(2)	0.00447(7)
As3	As, 33	0.39276(2)	0.64082(2)	0.35164(2)	0.00808(8)
Ca1a	Ca, 3.0(4)	0.1527(8)	0.1527(8)	0.1527(8)	0.0020(2)
Ca1b	Ca, 17.0(4)	0.1634(2)	0.1634(2)	0.1634(2)	0.0020(2)
Ca2	Ca 20.20(6)	0.09341(3)	0.62516(3)	0.35630(3)	0.0064(1)
Ti	(Ti,Fe), 24.6(1)	0.95176(4)	0.75	0.25	0.0036(2)
Fe1	Fe, 10.92(5)	0.2398(11)	0.75	0.75	0.0023(2)
Fe2	Fe, 21.35(5)	-0.00609(4)	0.25	0.25	0.0022(2)
Mn1	(Mn,Fe), 25.5(1)	0	0	0	0.0053(2)
O1	O, 8	-0.0055(1)	0.9813(1)	0.1370(1)	0.0077(5)
O2	O, 8	0.3097(1)	0.0036(1)	0.3598(1)	0.0080(5)
O3	O, 8	0.2879(1)	0.6331(1)	0.0477(1)	0.0083(5)
O4	O, 8	0.1637(1)	0.7378(1)	0.1456(1)	0.0094(5)
O5	O, 3.26(1)	0.1644(4)	0.5814(4)	0.2126(4)	0.0111(6)
O5'	O, 4.74 (1)	0.1801(3)	0.6031(3)	0.2288(3)	0.0111(6)
O6	O, 8	0.0325(1)	0.6639(1)	0.2256(1)	0.0086(5)
O7	O, 4.1(2)	0.1666(6)	0.4253(6)	0.2117(3)	0.0076(6)
O7'	O, 3.9(2)	0.1805(6)	0.4094(6)	0.2153(3)	0.0076(6)
F	F, 8.8(2)	0.75	0.75	0.75	0.0115(10)
NDSC					
As1	As, 33	0.37653(6)	0.37653(6)	0.37653(6)	0.0079(2)
As2	As, 33	0.22919(6)	0.97788(5)	0.03858(5)	0.0073(2)
As3	As, 33	0.39291(6)	0.64070(6)	0.35185(6)	0.0110(2)
Ca1	Ca, 20	0.16224(9)	0.16224(9)	0.16224(9)	0.0118(2)
Ca2	Ca, 20	0.09364(8)	0.62529(8)	0.35598(8)	0.0092(3)
Ti	(Ti,Fe), 21.0(2)	0.95129(15)	0.75	0.25	0.0073(6)
Fe1	Fe, 15.4(2)	0.25	0.75	0.75	0.0236(8)
Fe2	(Fe,Ti), 21.9(3)	0.00607(7)	0.25	0.25	0.0065(8)
Mn1	(Mn,Fe), 25.3(2)	0	0	0	0.0099(3)
O1	O, 8	-0.00570(7)	0.98121(6)	0.13718(7)	0.0107(2)
O2	O, 8	0.30994(7)	0.00363(7)	0.35999(6)	0.0108(2)
O3	O, 8	0.28798(7)	0.63273(6)	0.04786(7)	0.0120(3)
O4	O, 8	0.16361(7)	0.73782(6)	0.14472(7)	0.0131(3)
O5	O, 8	0.17414(10)	0.59523(12)	0.22296(10)	0.0385(5)
O6	O, 8	0.03262(7)	0.66448(7)	0.22564(7)	0.0122(3)
O7	O, 8	0.17329(8)	0.41758(8)	0.21302(8)	0.0200(3)
F	F, 9	0.75	0.75	0.75	0.0135(4)

Note: Mixed X-ray scattering factors (in *XRDSC-1* and *XRDSC-2*), or neutron scattering lengths (in *NDSC*) were used to model the *Mn1* and *Ti* sites. For the *Fe1* and *Fe2* sites, only the X-ray scattering factor/neutron scattering length of Fe were used. Bond valences calculated with the routine implemented in JANA2006. XRDSC-1 and XRDSC-2 represent two different X-ray refinements based on different protocols; details are given in the section *"Results: X-ray and neutron structure refinement"*.

Table 4. Refined displacement parameters (Å^2) in the expression: $-2\pi^2[(ha^*)^2U_{11} + \ldots + 2hka^*b^*U_{12} + \ldots + 2klb^*c^*U_{23}]$, based on the X-ray (XRDSC) and neutron (NDSC) structure refinements (see Table 3 for details).

	U_{11}	U_{22}	U_{33}	U_{12}	U_{13}	U_{23}
XRDSC-1						
As1	0.00541(9)	0.00541(9)	0.00541(9)	0.00145(9)	0.00145(9)	0.00145(9)
As2	0.0051(1)	0.0041(1)	0.0041(1)	-0.00095(9)	-0.00038(9)	0.00027(8)
As3	0.0117(1)	0.0057(1)	0.0068(1)	-0.00045(9)	0.0041(1)	0.00077(9)
Ca2	0.0060(3)	0.0069(3)	0.0063(3)	-0.0021(2)	-0.0008(2)	0.0003(2)
Ti	0.0029(3)	0.0047(3)	0.0035(3)	0	0	0.0012(2)
Fe1	0.087(1)	0.0030(5)	0.0092(5)	0	0	0
Fe2	0.0012(3)	0.0027(3)	0.0030(3)	0	0	-0.0015(2)
Mn1	0.0052(3)	0.0052(3)	0.0052(3)	0.0014(2)	0.0014(2)	0.0014(2)
O1	0.0091(9)	0.0055(9)	0.0080(9)	0.0033(7)	0.0000(7)	-0.0024(7)
O2	0.0113(9)	0.0096(9)	0.0032(8)	-0.0017(7)	-0.0013(7)	0.0018(7)
O3	0.0106(9)	0.0032(8)	0.0109(9)	0.0011(7)	-0.0019(7)	-0.0009(7)
O4	0.0085(9)	0.0075(9)	0.0123(9)	0.0000(7)	0.0046(7)	0.0015(7)
O5	0.036(2)	0.054(2)	0.039(2)	0.035(1)	0.021(1)	0.034(1)
O6	0.0074(9)	0.0095(9)	0.0083(9)	0.0027(7)	0.0029(7)	0.0009(7)
O7	0.025(1)	0.028(1)	0.009(1)	-0.0177(9)	0.0011(8)	-0.0077(8)
F	0.009(2)	0.009(2)	0.009(2)	0	0	0
XRDSC-2						
As1	0.00540(9)	0.00540(9)	0.00540(9)	0.00145(9)	0.00145(9)	0.00145(9)
As2	0.0051(1)	0.0041(1)	0.0042(1)	-0.00093(9)	-0.0004(1)	0.00026(9)
As3	0.0116(1)	0.0058(1)	0.0068(1)	-0.0004(1)	0.0041(1)	0.0008(1)
Ca2	0.0060(3)	0.0070(3)	0.0063(3)	-0.0021(2)	-0.0008(2)	0.0004(2)
Ti	0.0028(3)	0.0047(3)	0.0032(3)	0	0	0.0012(2)
Fe1	0.057(7)	0.0027(5)	0.0090(6)	0	0	-0.002(1)
Fe2	0.0011(3)	0.0027(3)	0.0030(3)	0	0	-0.0015(2)
Mn1	0.0053(3)	0.0053(3)	0.0053(3)	0.0015(2)	0.0015(2)	0.0015(2)
O1	0.0091(9)	0.0054(9)	0.008(1)	0.0034(7)	0.0002(7)	-0.0023(7)
O2	0.012(1)	0.0095(9)	0.0032(9)	-0.0017(7)	-0.0015(7)	0.0017(7)
O3	0.0110(9)	0.0032(9)	0.0108(9)	0.0013(7)	-0.0016(7)	-0.0009(7)
O4	0.0088(9)	0.0077(9)	0.012(1)	-0.0001(7)	0.0041(7)	0.0014(7)
O6	0.0075(9)	0.0097(9)	0.0086(9)	0.0027(7)	0.0028(7)	0.0007(7)
F	0.012(2)	0.012(2)	0.012(2)	0	0	0
NDSC						
As1	0.0079(3)	0.0079(3)	0.0079(3)	0.0015(3)	0.0015(3)	0.0015(3)
As2	0.0081(4)	0.0071(3)	0.0068(3)	-0.0008(3)	-0.0002(3)	0.0003(3)
As3	0.0150(4)	0.0088(4)	0.0092(4)	0.0001(3)	0.0041(3)	0.0010(3)
Ca1	0.0118(4)	0.0118(4)	0.0118(4)	0.0022(5)	0.0022(5)	0.0022(5)
Ca2	0.0084(5)	0.0103(5)	0.0090(5)	-0.0021(4)	-0.0003(4)	0.0000(4)
Ti	0.0044(11)	0.0126(12)	0.0049(11)	0	0	0.0026(9)
Fe1	0.055(2)	0.0066(11)	0.0096(11)	0	0	0
Mn1	0.0099(6)	0.0099(6)	0.0099(6)	0.0012(4)	0.0012(4)	0.0012(4)
O1	0.0112(4)	0.0086(4)	0.0124(4)	0.0024(4)	-0.0005(4)	-0.0023(4)
O2	0.0137(4)	0.0115(4)	0.0072(4)	-0.0004(4)	-0.0015(4)	0.0014(4)
O3	0.0146(4)	0.0068(4)	0.0147(4)	0.0017(4)	-0.0013(4)	0.0003(4)
O4	0.0130(4)	0.0101(4)	0.0160(5)	0.0003(4)	0.0067(4)	0.0020(4)
O5	0.0338(8)	0.0488(9)	0.0328(8)	0.0318(7)	0.0177(6)	0.0298(7)
O6	0.0103(4)	0.0130(5)	0.0133(4)	0.0030(3)	0.0033(4)	0.0019(4)
O7	0.0233(6)	0.0257(6)	0.0110(5)	-0.0153(5)	0.0014(4)	-0.0062(4)
F	0.0135(7)	0.0135(7)	0.0135(7)	0	0	0

Note: XRDSC-1 and XRDSC-2 represent two different X-ray refinements based on different protocols; details are given in the section *"Results: X-ray and neutron structure refinement"*.

Table 5. Relevant bond distances (Å) and angles (°) based on the X-ray and neutron structure refinement of cafarsite (see Table 3 for details).

XRDSC-1			XRDSC-2			NDSC		
As1-	O7 x 3	1.765(7)	*As1-*	O7 x 3	1.746(7)	*As1-*	O7 x 3	1.761(1)
				O7' x 3	1.802(7)			
As2-	O1	1.750(2)				*As2-*	O1	1.749(1)
	O2	1.785(2)	*As2-*	O1	1.750(2)		O2	1.782(3)
	O3	1.795(2)		O2	1.785(2)		O3	1.792(1)
				O3	1.796(2)			
As3-	O4	1.791(2)				*As3-*	O4	1.793(1)
	O5	1.753(3)	*As3-*	O4	1.791(2)		O5	1.759(2)
	O6	1.754(3)		O5	1.664(7)		O6	1.756(1)
				O5'	1.830(5)			
Ca1a-	O2 x 3	2.460(4)		O6	1.752(2)	*Ca1-*	O2 x 3	2.593(2)
	O7 x 3	2.434(6)					O7 x 3	2.369(2)
	F	2.688(6)	*Ca1a-*	O2 x 3	2.461(14)		F	2.425(1)
				O7 x 3	2.507(15)			
Ca1b-	O2 x 3	2.611(2)		O7' x 3	2.365(15)	*Ca2-*	O1	2.326(2)
	O7 x 3	2.357(3)		F	2.687(14)		O1	2.516(2)
	F	2.393(2)					O2	2.569(2)
			Ca1b-	O2 x 3	2.611(3)		O3	2.435(2)
Ca2-	O1	2.320(2)		O7 x 3	2.446(8)		O3	2.653(2)
	O1	2.514(2)		O7' x 3	2.270(8)		O4	2.452(2)
	O2	2.570(2)		O7' x 3	2.871(10)		O5	2.526(2)
	O3	2.439(2)		F	2.392(2)		O6	2.379(2)
	O3	2.649(2)						
	O4	2.457(2)	*Ca2-*	O1	2.320(2)	*Ti-*	O3 x 2	1.966(1)
	O5	2.539(3)		O1	2.513(2)		O4 x 2	2.069(2)
	O6	2.381(2)		O2	2.571(2)		O6 x 2	1.922(2)
				O3	2.439(2)			
Ti-	O3 x 2	1.961(2)		O3	2.650(2)	*Fe1-*	O4 x 4	2.181(1)
	O4 x 2	2.083(2)		O4	2.457(2)		O5 x 4	2.783(2)
	O6 x 2	1.922(2)		O5	2.657(7)			
				O5'	2.485(5)	*Fe2-*	O2 x 2	2.004(3)
Fe1-	O4 x 4	2.168(2)		O6	2.380(2)		O5 x 2	1.916(4)
	O5 x 4	2.791(3)					O7 x 2	1.959(3)
			Ti-	O3 x 2	1.960(2)			
Fe2-	O2 x 2	2.001(2)		O4 x 2	2.083(2)	*Mn1-*	O1 x 6	2.210(1)
	O5 x 2	1.913(4)		O6 x 2	1.925(2)			
	O7 x 2	1.956(3)						
			Fe1-	O4 x 2	2.201(2)			
Mn1-	O1 x 6	2.208(2)		O4 x 2	2.160(2)			
				O5 x 2	2.886(8)			
				O5' x 2	2.831(5)			
				O5' x 2	2.422(5)			
			Fe2-	O2 x 2	2.000(2)			
				O5 x 2	1.915(7)			
				O5' x 2	1.935(5)			
				O7 x 2	1.951(9)			
				O7' x 2	1.979(10)			
			Mn1-	O1 x 6	2.207(2)			

Note: XRDSC-1 and XRDSC-2 represent two different X-ray refinements based on different protocols; details are given in the section *"Results: X-ray and neutron structure refinement"*.

Figure 1. Representative single-crystal Raman spectrum of the cafarsite sample of this study (un-oriented crystal).

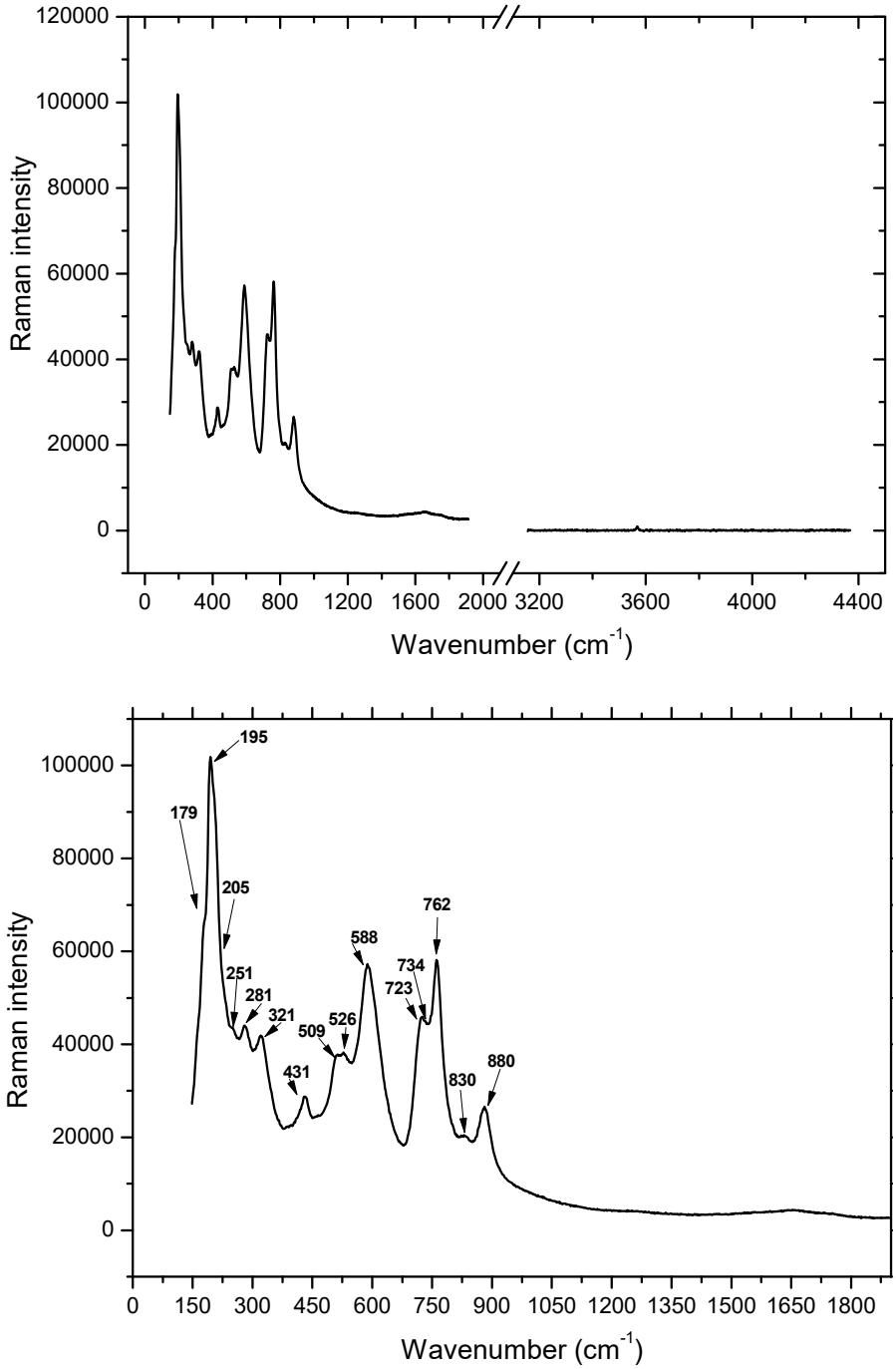

Figure 2. The crystal structure of cafarsite viewed down [001], based on the X-ray structure refinement of this study. Four additional clinographic views, with the polyhedra configurations, are shown. Atomic displacement probability factor: 50%.

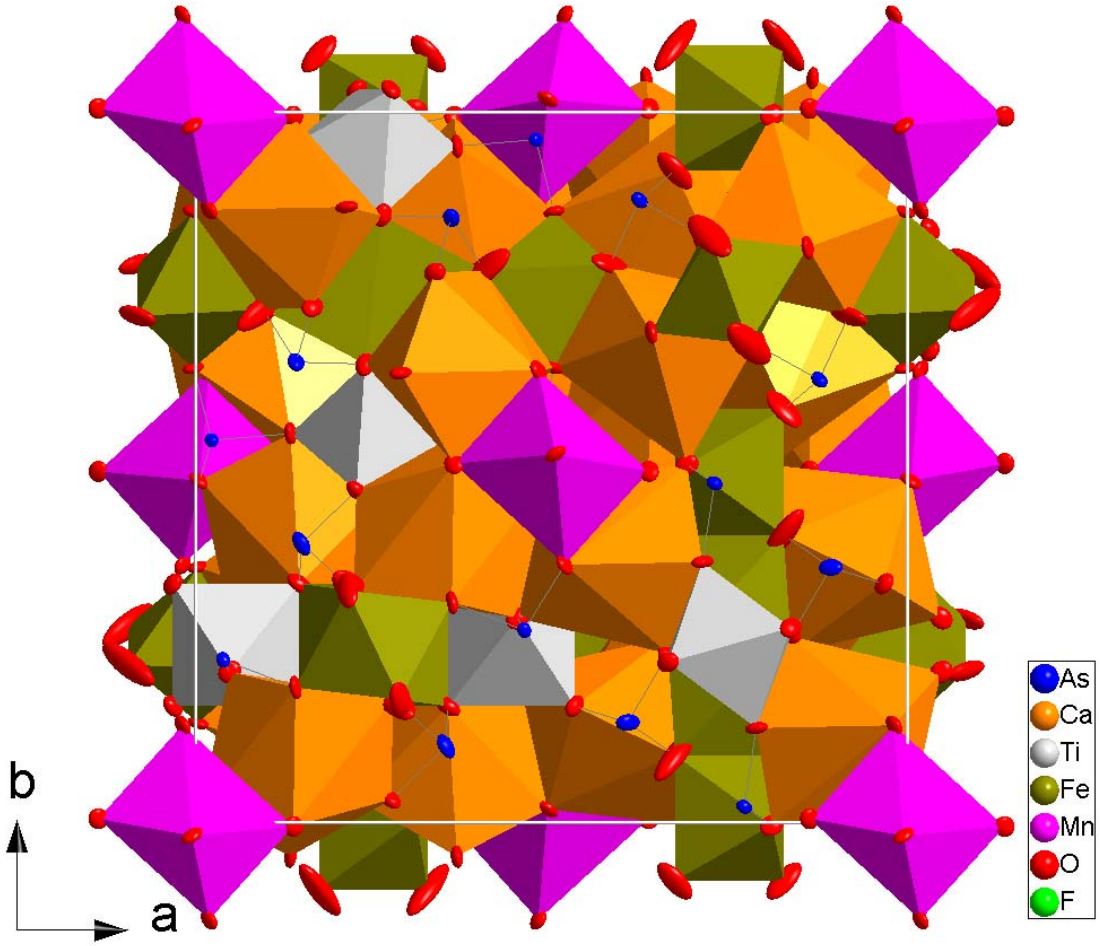

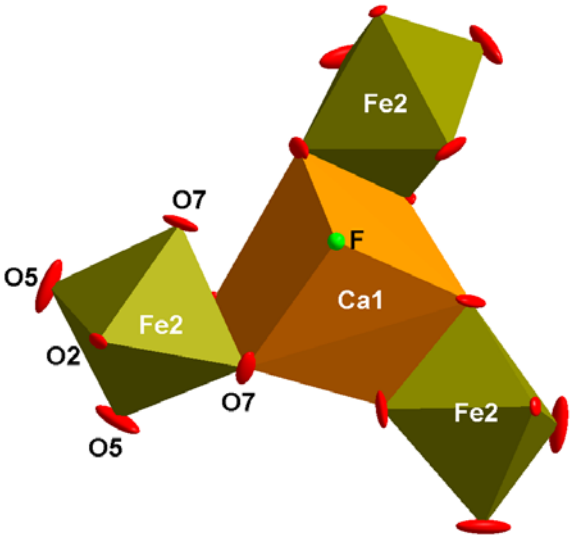
Fe2
O7
F
O5
Fe2
Ca1
O2
O7
Fe2
O5

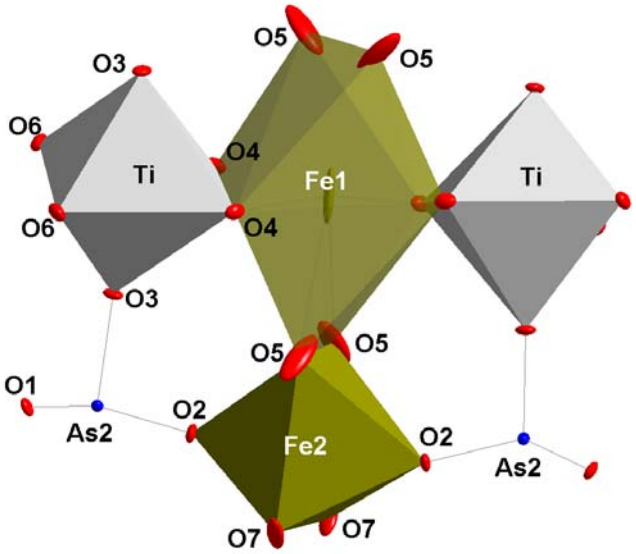
O5
O3
O5
O6
Ti
O4
Fe1
Ti
O6
O4
O3
O5
O5
O1
O2
As2
Fe2
O2
As2
O7
O7

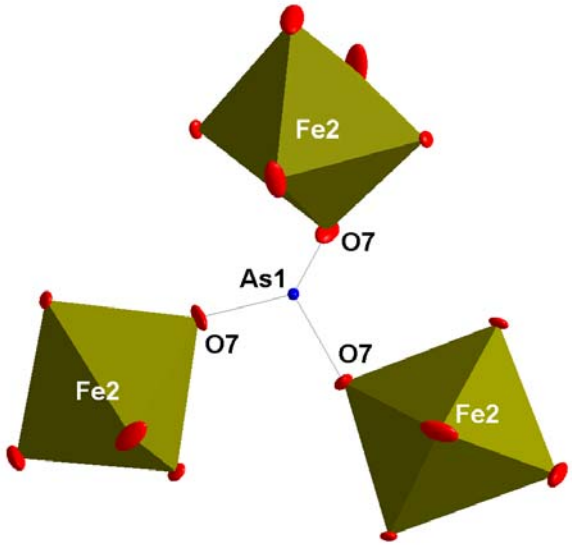
Fe2
O7
As1
O7
O7
Fe2
Fe2

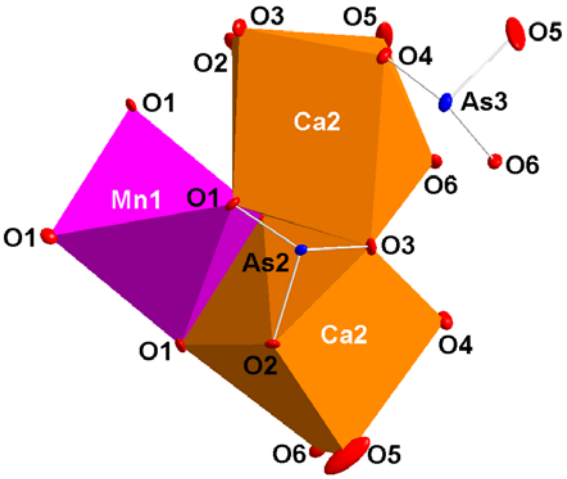
O3
O5
O5
O2
O4
O1
Ca2
As3
O6
O6
Mn1
O1
O1
O3
As2
Ca2
O4
O1
O2
O6
O5